COMMUNICATIONS OF COMPUTATIONAL FLUID DYNAMICS, NO. 3, PP. 49-69, 2004
HTTP://CFDCHINA.COM

COMPARISONS OF STEADY AND TIME AVERAGED UNSTEADY ANALYSIS RESULTS FOR IMPELLER AND VANED DIFFUSER INTERACTIONS IN A CENTRIFUGAL COMPRESSOR STAGE

N.HE, A.TOURLIDAKIS AND R.L.ELDER

ABSTRACT

In this paper, a computational analysis of the interactions between a backswept impeller and its downstream vaned diffuser in a high-speed centrifugal compressor is presented. Both steady and unsteady simulations are carried out at peak efficiency and emphasis is focused on the comparison between steady and time averaged unsteady simulation results. In addition, some unsteady phenomena are discussed in order to advance our understanding of the flow physics. One important conclusion is that generally, there is a good agreement between the steady and time averaged results, however, the difference is relatively larger in the velocity field and stage efficiency, therefore the unsteady simulation is still important.

INTRODUCTION

The flow in the region between the impeller tip and the vaned diffuser leading edge inside a centrifugal compressor stage is complex, highly viscous and contributes to a significant amount of aerodynamic losses.

The flow field is physically unsteady and in order to have a better understanding of the flow in this region, it is important to analyse the unsteady interaction between the impeller and the downstream vaned diffuser. The simulation of the fully unsteady flow requires extensive computational resources, and there is a need to define if and when the use of these resources is justified.

A major problem in the unsteady simulation is that when the number of rotor and stator blades is different, the flow is not the same through each blade channel. In the most general case, all blade passages of the stator and rotor have to be modelled leading to a very expensive calculations. There are several methods to economically address the unequal pitch problem but these methods do introduce limitations.

Rai (1987) published an approach based on geometry scaling, which addresses the problem of unequal pitch by modifying the geometry to the nearest integer pitch ratio. The advantages of this method are that it is relatively simple and much less computationally expensive than other methods. The main disadvantage of this method is that it is less accurate because it physically changes the number of blades for the actual configuration. If appropriately applied, however, the influence of these changes can be minimised and because of the computational resources currently available, this method has been used in this study.

Another method was proposed by Erdos (1977) which is known as Periodic Phase Shifting. In this method, a phase shift is introduced in applying the periodic boundary conditions. The advantage of this method is its ability to deal with an arbitrary pitch ratio without scaling the geometry as for Rai's method. This method has the

advantage of calculating the stator and rotor fields at the same time step, making the numerical algorithm less complex. One of the main disadvantages of this method is that it is less robust.

A third method introduced by Giles (1990) known as the Time Inclined method inclines the computational grid in time, automatically satisfying the lagged periodic boundary. This method allows the application of simple periodicity conditions on small computational domains independently of the stage's pitch ratio and without modifying or scaling geometry, and hence it is more accurate. The disadvantage of this method is that the implementation of the numerical algorithm becomes much more complex.

In recent years, various researchers used different CFD solvers or carried out experimental work in order to investigate the interactions between impeller and vaned diffuser. Dawes (1995) presented a time-resolved simulation of the Krain centrifugal impeller-diffuser interaction using a time-accurate, three-dimensional, unstructured mesh Navier-Stokes solver. The predicted flow field, compared with experimental data, confirmed a complex, highly distorted three-dimensional flow in the entry zone to the diffuser. Koumoutsos et al (2000) analysed the same stage with the pressure-based solver TASCflow and provided detailed comparisons between computational and experimental data in the interaction region. Justen et al (1999) published an experimental investigation of unsteady flow phenomena in a centrifugal compressor in order to estimate the influence of the unsteadiness on the operating performance of the stage. Shum et al (2000) showed that the most influential aspect of the unsteady interaction between centrifugal impeller and diffuser was the effect on impeller tip

leakage flow and that there was an optimal radial gap size for maximum impeller pressure rise.

In this paper, both unsteady and steady simulations are carried out in order to analyse the interactions between a centrifugal impeller and its downstream vaned diffuser. The main emphasis is focused on the comparisons between the time averaged unsteady results and its steady simulation results. The steady state assumption is still widely used in the CFD simulations and designers utilize the steady results as guidance during the design process. However, it is essential to quantify the differences between the averaged unsteady simulation results and the steady state results in order to assess what the penalty of the steady state assumption involves. Therefore, this work could provide some useful information for the designers who employ steady state methods as to when it is necessary to take into account the effects of unsteadiness.

NOMENCLATURE

L/W	diffuser length to throat width ratio
AS.R	aspect ratio
A.R	area ratio
k	turbulent kinetic energy
ε	turbulent dissipation rate
α	2D incidence angle (°)
β	leading edge angle (°)
γ	flow angle (°)

VR vane radius (mm)

TR radius ratio of the trailing edge of diffuser to the impeller tip

NUMERICAL METHOD

The computational analysis uses the commercial CFD code CFX-TASCflow (10) which solves the three-dimensional Reynolds-Averaged Navier-Stokes equations in rotating and/or stationary frames of reference. In the present study, the standard k-ε turbulence model with wall functions was used. A pressure correction method is employed for the coupling of the continuity and the momentum equations and the update of the pressure field. A finite volume method is employed for the discretization and an algebraic multigrid method is used for accelerating the solution procedure. The computational grid employed involves a structured boundary-fitted, generally non-orthogonal and curvilinear three-dimensional mesh. A non-staggered, collocated grid arrangement is used for the flow variables. A number of higher-order bounded differencing schemes are employed for the treatment of the convective terms. More details about the mathematical and numerical aspects of the method can be found in the software documentation (10).

GEOMETRY DEFINITION

The simulation was performed for a centrifugal compressor stage with a backswept impeller and a diffuser with 22 vanes. The computational programme aimed to simulate the experimental work carried out at Cranfield University by Foster (1987). The backswept impeller consisted of eight full and eight splitter blades. The tip diameter was equal to 101.6 mm and the inducer diameter was 71.1mm. The

backsweep at the impeller exit commenced at a radius of 37.5mm and the backsweep angle (from radial direction) varied from 13.5° at the shroud to 27° at the hub at the exit of the impeller. A Double Circular Arc vane generation method was used for the diffuser vane profiles, whereby the suction and pressure surfaces of the diffuser blades were generated by two circular arcs of the same radius but displaced centre. More detailed design information for the diffusers is given in Table 1.The radius ratio is relative to the impeller tip and the geometric throat area was 667.49 mm^2.

No of Vanes	22
L/W	8.25
AS.R	1.45
A.R	2.16
α	8.4
β	74.9
VR	168.275
RR	1.075
TR	1.6125

Table 1. Design information of the vaned diffuser tested

GEOMETRY SCALING, COMPUTATIONAL GRID AND BOUNDARY CONDITIONS

For the unsteady simulation, the vaned diffuser is approximated as having 24 blades instead of 22 as in the actual configuration. One passage of the impeller and three passages of the vaned diffusers are used for the unsteady simulation. For this reason, the vaned diffuser geometry needs to be scaled, and this has been performed by reducing the thickness of the blade by a factor of 22/24 in order to maintain the throat area of the actual configuration. During the geometry scaling, the co-ordinates of the centre of the circular arcs forming the suction and pressure sides remained the same,

whereas the radius of the arc of the suction side was increased in order to obtain the required thickness of the vane. During the geometry scaling, the inlet flow direction and the outlet to inlet area ratio of the diffuser were kept unchanged.

After the completion of the geometry definition and scaling, separate grids were generated for the impeller and the scaled diffuser geometry, Figure 1. Turbogrid (1998) was used for the grid generation, which is appropriate for domains with periodic boundaries. The grids used were structured grids of H-type.

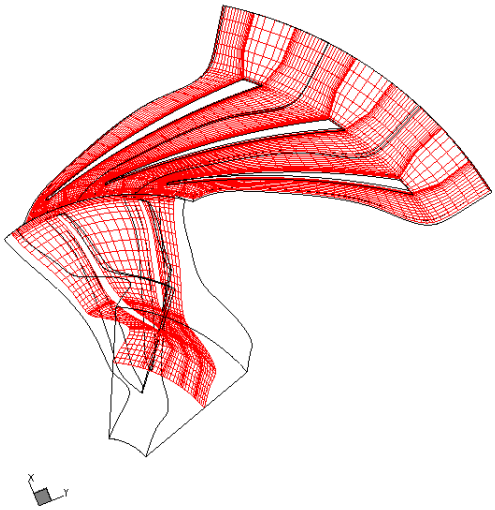

Figure 1. Computational grids for the unsteady simulation

The unsteady simulation is quite expensive and time-consuming, and consequently relatively coarse grids were employed. The impeller grid consisted of 50 points in the streamwise direction, 40 points in the tangential direction and 20 grid nodes from hub to the shroud giving a total of 40,000 grid points. For one vaned diffuser passage, the grid consisted of 40 points in the streamwise, 35 points in the circumferential and 20 points in the spanwise direction providing a total of 28,000 grid points. The total number of grid nodes used for the stage analysis (one full impeller and three diffuser passages) was 124,000.

An important step is to define the interface between the exit of the rotational impeller and the inlet of the stationary vaned diffuser. The condition at the interface was fixed to “rotor/stator”, which is a sliding interface approach used in the real transient simulation. In the unsteady simulation, the true transient interaction of the flow between an impeller and vaned diffuser passage and the relative motion between the two components are simulated and this approach ultimately accounts for all interaction effects.

In order to compare the differences between the results from the steady and unsteady simulations, both were carried out on the same scaled geometry, grid size and boundary conditions. The only difference is that for the steady analysis, the interface between the impeller outlet and the vaned diffuser inlet changes to the “stage averaging” condition. Using this condition involves circumferential averaging of the velocity components as they are transformed from the rotating to the stationary frame of reference whereas the potential fields are free to develop independently from both sides of the interface.

RESULTS AND DISCUSSIONS

Time Step Refinement

The unsteady simulation was carried out inside the centrifugal compressor stage with the impeller’s rotational speed fixed at 75,000 rpm and for the peak efficiency condition at a mass flow rate of 0.41 kg/s. The period of every diffuser passage is $\Delta T = 1/(3\times 8)/(75{,}000/60) = 3.3333\times 10^{-5}$ s. Every diffuser passage was modelled

with 10 time steps, and hence the time step is equal to $3.3333 \times 10^{-6} s$. Every full impeller passage needs 30 time steps.

In order to monitor the developing solution, several monitoring points were selected in various locations of the flow domain. These points can be used to track the progress of the solution from one time step to the next and to determine whether a repeating cycle has been established.

Some results were obtained at the above defined time step. From the plots of the variations of static pressure, u, v and w velocity components for the pre-selected monitoring points (Figure 2 shows the monitoring point 2, which is near to the leading edge of vaned diffuser at midspan), it can be seen clearly that most of the plots for the velocity fields have substantially established repeating patterns, but this is not always the case from the plots of the static pressure.

For this reason, time step refinement was undertaken in order to quantify the effects of the time step selection on the results. The time step was decreased to half of the original time step value to $1.66665 \times 10^{-6} s$.

The same monitoring points were used for the small time step and it was observed that, both velocity and static pressure fields established a repeating pattern.

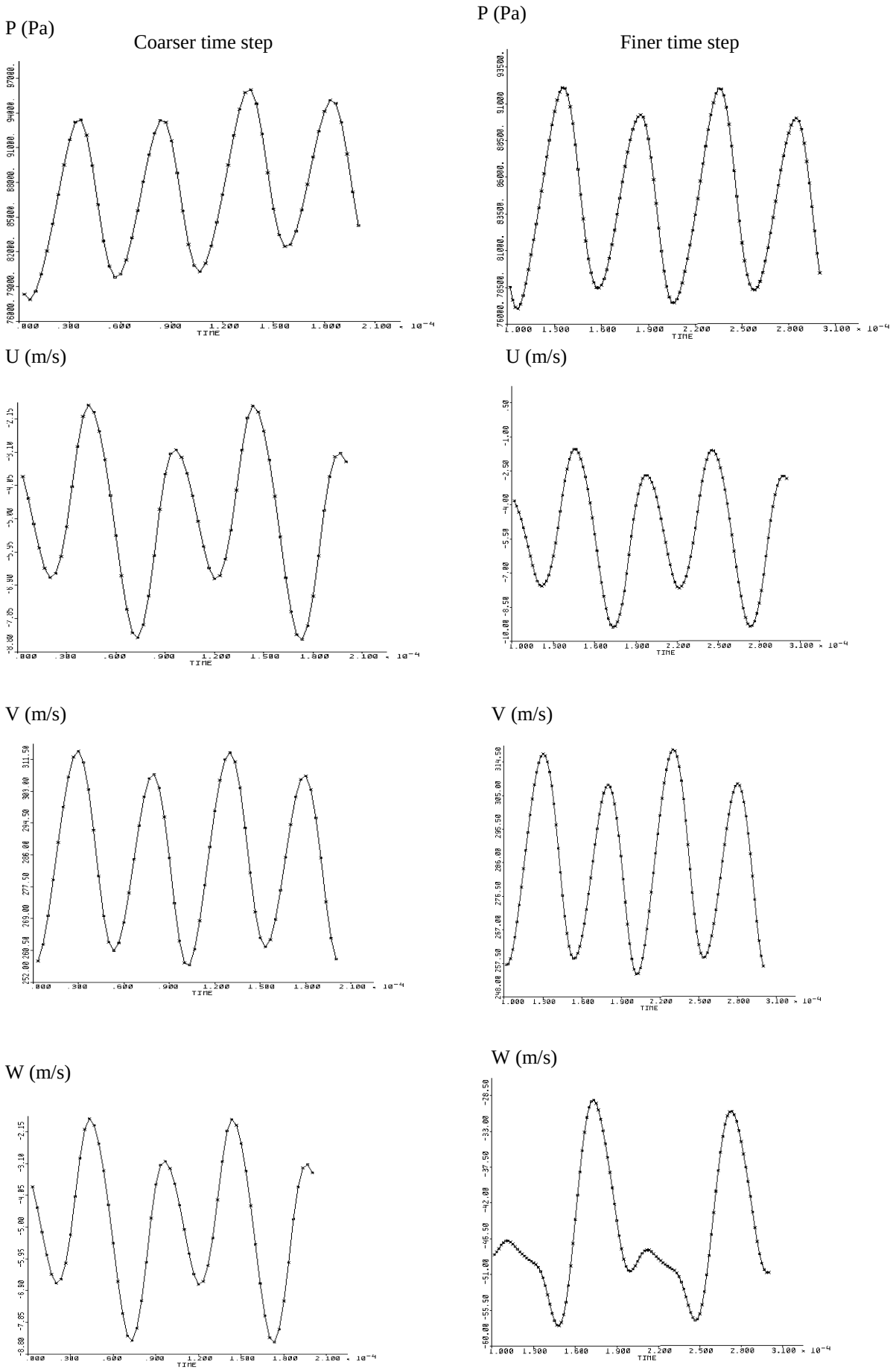

Figure 2. Comparison of the Variations of static pressure, u, v, w velocity at the monitoring point 2 (near leading edge, midspan) between two time steps

Comparisons between unsteady predicted results and experimental data

(velocity vectors and isentropic efficiency)

Experimental data was available providing the velocity vectors at 11 points in the throat area, semi-vaneless space and vaneless space of the vaned diffuser. These points are dissipated D, E, F, G, H, J, K, L, M, N, P in Figure 3. At each of these stations, measurement were available, near the casing wall (25% blade height), the midspan (50% blade height) and the hub (75% blade height). All values of velocity magnitude are normalised to the impeller tip speed. Figures 3 presents comparisons between the experimental data and predicted results for the velocity vectors at a particular location of the impeller relatively to the diffuser. The velocity vectors with colours represent predicted results.

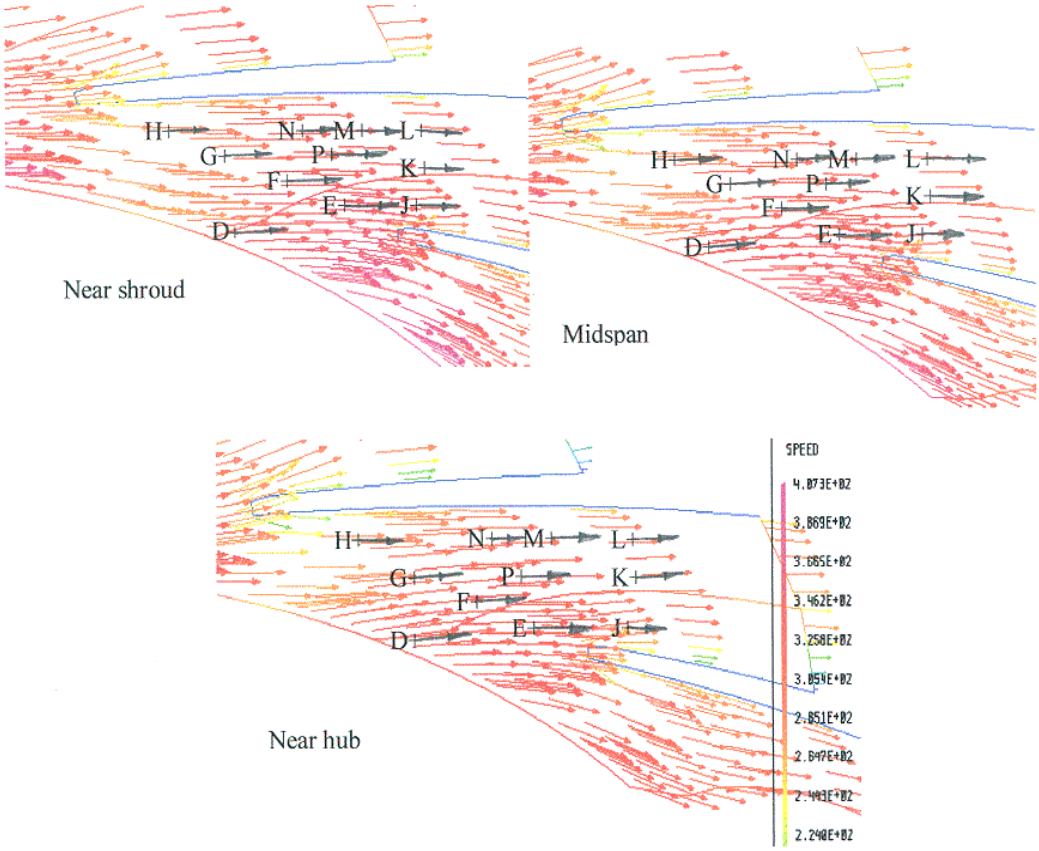

Figure 3. Comparison of the Velocity vectors between the predicted results and experimental data.

From the comparisons of velocity vectors (both direction of velocity and magnitude of velocity), the predicted results appear quite similar to the experimental data, implying that the current computational model for the unsteady simulation is reliable and the geometry scaling method used in the unsteady simulation is reasonable. It is also clear that the flow fields are highly unsteady with significant variations in the velocity field (both the magnitudes and flow directions).

The predicted isentropic efficiency of the averaged unsteady results is 74.68 % (exit of vaned diffuser), corresponding to an experimentally defined value of 74.31% (exit of scroll). The above comparison demonstrates that the predicted stage efficiency is quite similar to the experimental data.

Comparisons between time averaged unsteady simulation results and steady state simulation results

This investigation is based on the same scaled configuration, turbulence model and the number of grid nodes using steady and unsteady methods. The comparison is carried out in terms of static and total pressure, flow velocity and isentropic efficiency. A computer program was developed to post-process the computational results and compare the differences between the steady and time-averaged unsteady simulation results. In this paper only the most representative results will be presented.

Firstly, a comparison of the absolute total pressure at the vaned diffusers exit planes is presented, Figure 4. In general, there is a good agreement between the steady and

time-averaged unsteady simulation results although it appears that the flow is more uniform for the averaged unsteady results.

Figure 5 shows the difference in the local value of static pressure as predicted by the steady and the unsteady simulation at blade midspan. It is clear that the main differences occur in the area of the vaneless and semi-vaneless space. The maximum difference is about 0.12 bar (about 7% of the average pressure in this region). At the throat area and further downstream, the differences are quite small, around 0.01 bar (about 1% of the average pressure in this region).

Thirdly, the difference of the local velocity magnitude between the steady and averaged unsteady results at midspan are illustrated in Figure 6. It can be found that the main differences not only occur in the area of the vaneless space and semi-vaneless space but entered into the passage of the vaned diffuser. The maximum difference is about 16 m/s, which represents approximately 6% of the average speed in these regions.

A comparison of the different values of the absolute total pressure and flow angle at the impeller exit, the leading edge of the vaned diffuser and the vaned diffusers exit are given in Table 2.

	ΔP_{total}	$\Delta\gamma$
Impeller exit	0.20 bar (5.0% local value)	1.5°
Leading edge of vaned diffuser	0.25bar (5.5% local value)	2.0°
Vaned diffuser exit	0.01 bar (0.4% local value)	1.0°

$\Delta = |$ steady state-time averaged unsteady results $|$

Table 2. Comparison between the steady and averaged unsteady simulation results

The predicted results for the isentropic efficiency is 74.68 % for the averaged unsteady results and 73.33% for the steady state prediction. The difference is 1.35 % which is significant but probably expected from these by different computations. The experimental data indicates on isentropic efficiency of 74.31%, but this is at the exit of scroll whereas the computations are for the exit of the vaned diffuser.

Overall the differences between the steady and unsteady calculations are felt to be modest, however, their importance must depend on the finesse required. It is also appreciated that some of the differences occur in critical regions (impeller/diffuser interface) and even small differences might lead to particularly changes in stability limits.

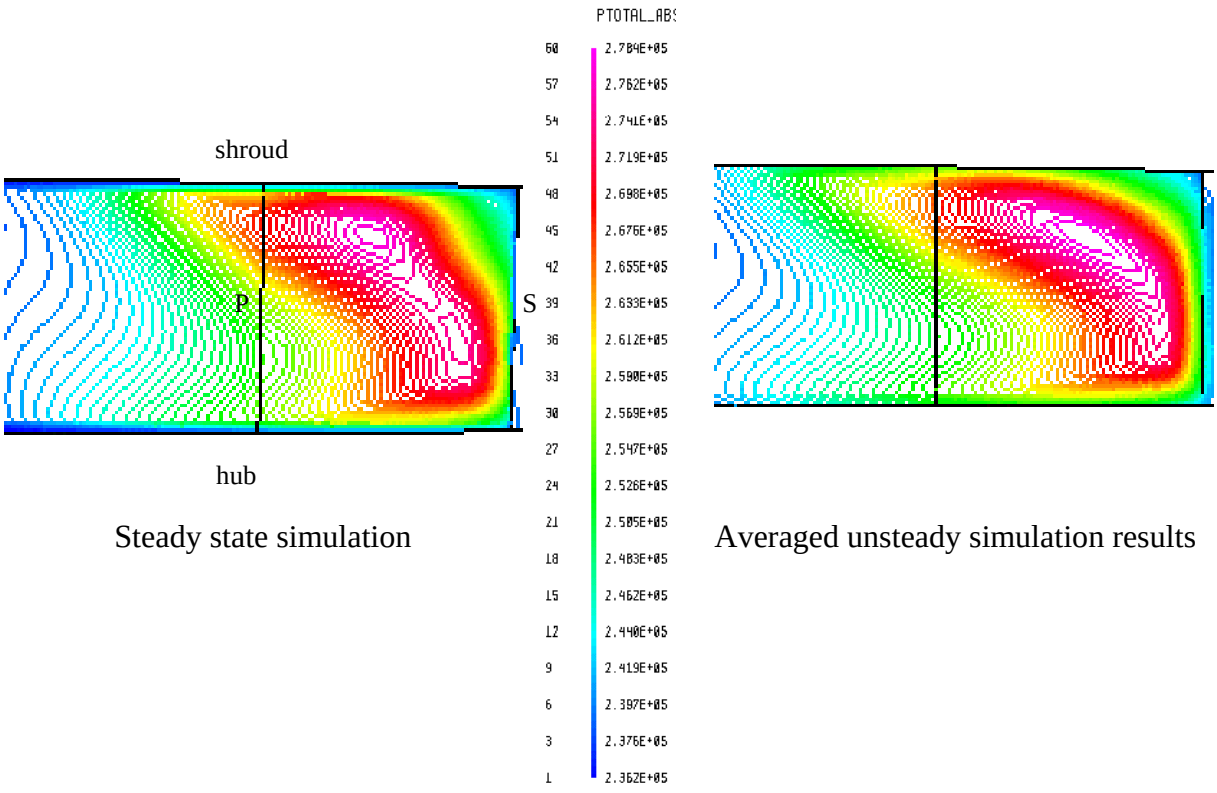

Figure 4. Absolute Total Pressure (Pa) at the Vaned Diffuser exit

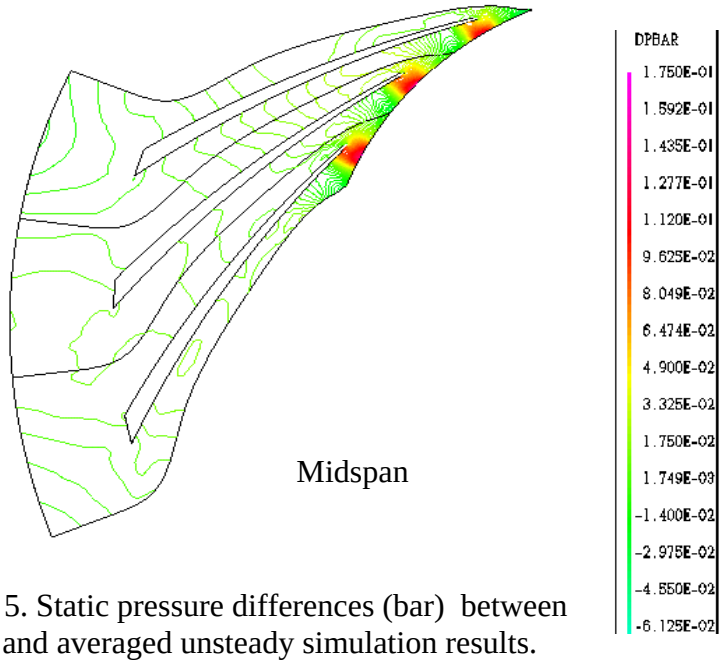

Figure 5. Static pressure differences (bar) between steady and averaged unsteady simulation results.

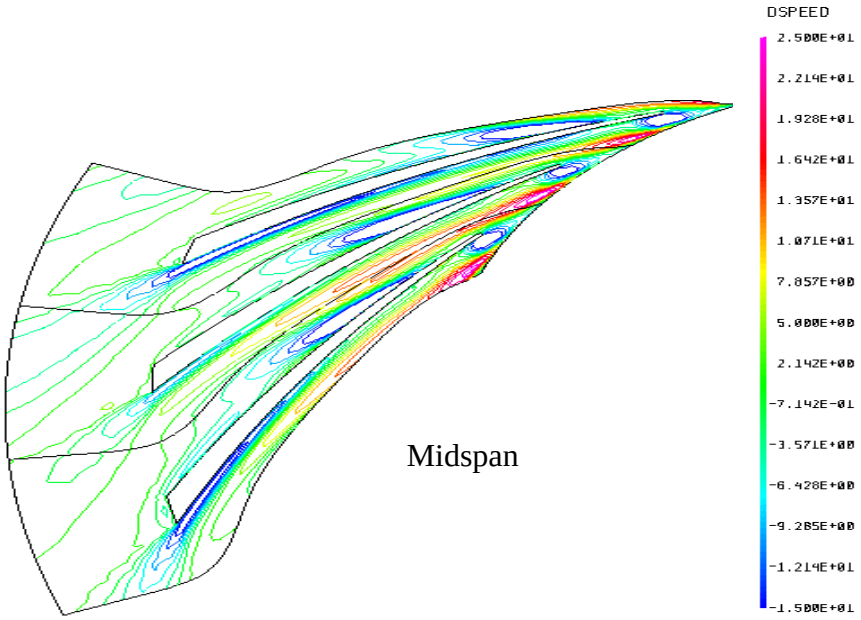

Figure 6. Velocity magnitude differences (m/s) between the steady results and averaged unsteady simulation results.

Level of Unsteadiness

The level of unsteadiness is an important parameter in the unsteady simulation because it directly reflects the magnitude of the variations of different flow variables. In order to know the level of the unsteadiness at different locations of the flow field, the value of the standard deviation of the unsteady variation was calculated.

If the time averaged flow variable is defined as $\bar{q} = \frac{1}{N}\sum_{n=1}^{N} q(n)$, where q(n) is the instantaneous values, then the standard deviation (rms-fluctuation) is given by $\tilde{q} = \sqrt{\frac{1}{N}\sum_{n=1}^{N}(q(n)-\bar{q})^2}$, where N is the number of the time steps in a period. A computer program was developed in order to post-process the simulation results and provide the standard deviations of the static pressure, velocity magnitude and total pressure at different computational planes.

Firstly, a comparison was carried out for the standard deviation of the static pressure at midspan (Figure 7). It can be observed that the maximum standard deviation of the static pressure occurs at the vaneless space and the level of unsteadiness rapidly decreases downstream in the diffuser passage. This is strong evidence that the flow in the diffuser inlet region is highly unsteady as might be expected due to the interaction of the stator vanes with the rotating impeller wakes.

The same comparison for velocity at blade midspan is shown in Figure 8. Again, maximum standard deviation occurs at the vaneless space and decreases further downstream. But in this case, the largest fluctuations are confined to the impeller tip region rather than the diffuser leading edge. Again, this supports our understanding of impeller flow with the impeller tip region being associated with a rapid mixing of the distorted outlet impeller flow.

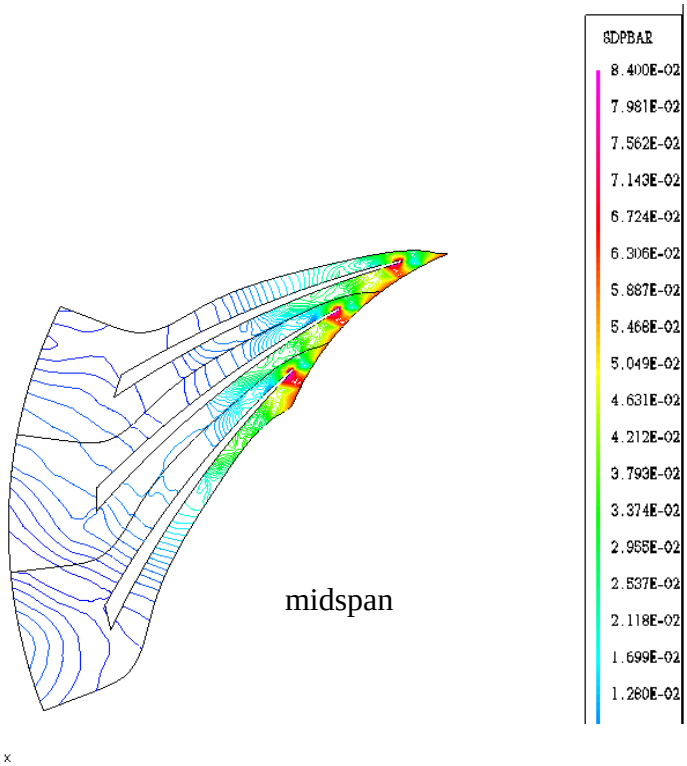

Figure 7. Standard deviation of the static pressure (bar) of the unsteady simulation

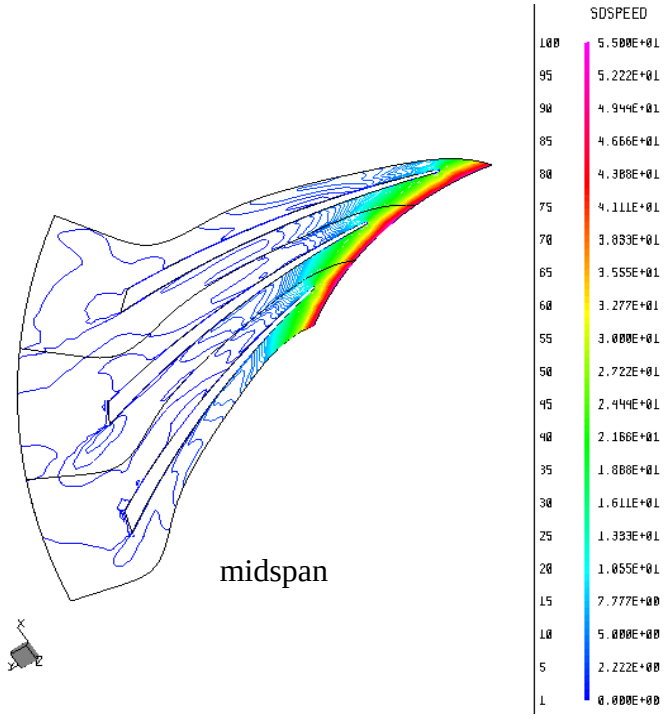

Figure 8. Standard deviation for the velocity magnitude (m/s) of the unsteady simulation.

CONCLUSIONS

From the comparisons of the predicted results and available experimental data, it is concluded that the geometry scaling method, used in the current unsteady simulation, is reasonablly successful and the computational model employed provides a significant representative of the actual flow field.

From the comparisons between time-averaged unsteady results and steady simulation results, it is observed that the differences are modest but could be important. A problem is that the unsteady, steady and experimental results all agree reasonably, making it difficult to be very precise on the improved accuracy of the unsteady result. It is also difficult to be certain that very apparent improvement shown by the unsteady result is due to a better physical representation as it could be due to non-representative factors.

The unsteadiness induced by the interaction between impeller and vaned diffuser influences the pressure fields, velocity fields, flow angles or incidence angles very significantly, particularly in the impeller tip to diffuser that region. Clearly this has structural implications even if the aerodynamic implications are as yet unclear. The authors feel that considerably more work a range of cases and with different numerical model is required before conclusions can be achieved.

REFERENCES

1. "CFX-Turbogrid User Documentation Version 1.3", AEA Technology, Advanced Scientific Computing, Ontario, Canada, May 1998.

2. Dawes W.N., 1995, "A simulation of unsteady interaction of a centrifugal impeller with its vaned diffuser : flow analysis", Transactions of the ASME, Vol.117, No.2, pp.205-306.

3. Erdos J. I ., 1977 , " Numerical solution of periodic transonic flow through a fan stage", AIAA Journal , No.5, Nov, 1977

4. Forster C. P., 1987, "Application of laser anemometry to the measurement of flow in a small high speed centrifugal compressor". PhD thesis.

5. Giles M. B., 1990, "Stator/rotor interaction in a transonic turbine", J. Propulsion vol.6, No.5, Sep-Oct, 1990

6. Justen F., Ziegler K. U. and Gallus H.E., 1999, "Experimental investigation of unsteady flow phenomena in a centrifugal compressor vaned diffuser of variable geometry", ASME Journal of Turbomachinery, Vol. 121, pp. 763-771.

7. Koumoutsos A., Tourlidakis A. and Elder R L., 2000,
"CFD analysis of unsteady flow interactions in a centrifugal compressor stage", ASME paper No 2000-GT-460.

8. Rai M. M., 1987, " Unsteady three-dimensional Navier-Stokes simulations of Turbine Rotor-Stator Interaction", AIAA-87-2058

9. Shum Y. K. P., Tan C. S. and Cumpsty N.A., 2000,"Impeller-diffuser interaction in centrifugal compressor",
ASME paper No 2000-GT-0428

10. "TASCflow Theory Documenation, Version 2.4", Advanced Scientific Computing Ltd., Waterloo, Ontario, Canada, March 1995.